

RESEARCH ARTICLE

Hydroclimatic variability in Santiago (Chile) since the 16th century

Roberto Serrano-Notivoli¹  | Ernesto Tejedor²  | Pablo Sarricolea³  |
Oliver Meseguer-Ruiz⁴  | Mathias Vuille²  | Magdalena Fuentealba⁵  |
Martín de Luis⁶ 

¹Estación Experimental de Aula Dei, Consejo Superior de Investigaciones Científicas (EEAD-CSIC), Zaragoza, Spain

²Department of Atmospheric and Environmental Sciences, University at Albany, SUNY, Albany, New York

³Department of Geography, University of Chile, Santiago, Chile

⁴Departamento de Ciencias Históricas y Geográficas, Universidad de Tarapacá, Arica, Chile

⁵Instituto de Ecología y Biodiversidad, Santiago, Chile

⁶Departamento de Ciencias Biológicas, Instituto de Ecología y Biodiversidad, Santiago, Chile

Correspondence

Roberto Serrano-Notivoli, Estación Experimental de Aula Dei, Consejo Superior de Investigaciones Científicas (EEAD-CSIC), Zaragoza, Spain.
Email: rserrano@eead.csic.es

Funding information

Departament d'Universitats, Recerca i Societat de la Informació, Grant/Award Number: 2017SGR1362; Division of Atmospheric and Geospace Sciences, Grant/Award Number: AGS-1702439; Fondo de Fomento al Desarrollo Científico y Tecnológico, Grant/Award Number: AFB170008; Gobierno de Aragón, Grant/Award Number: Group H38; Ministerio de Ciencia e Innovación, Grant/Award Numbers: CAS/1900020, CGL2015-69985-R, CGL2017-83866-C3-2-R, FJCI-2017-31595; Office of International Science and Engineering, Grant/Award Number: OISE-1743738

Abstract

The long-term hydroclimatic variability in Santiago (Chile) was analysed by means of a new 481-year (1536–2016 CE) tree-ring reconstruction of the Standardized Precipitation Evapotranspiration Index (SPEI) of August, integrating the hydroclimatic conditions during the preceding 14 months. Results show a high frequency of extreme drought events in the late 20th and early 21st centuries, while the frequency of extreme wet events was higher in the 17th–18th centuries. The mid-20th century represents a breaking point for the hydroclimatic history in the region, including some significant changes: (a) the inter-annual variability increased; (b) the wet events became less intense; (c) the extreme dry events became more frequent; and (d) the most intense dry event of the entire period was identified, coinciding with the so-called Megadrought (2006–2016). A correlation analysis between the reconstructed SPEI and three climate indices (PDO, SOI and Niño3.4) was performed at monthly scale, considering different multi-annual aggregations. The analysis shows diverse impacts on the hydroclimatic variability, with positive correlations between SPEI and PDO as well as Niño3.4, and negative correlations between SPEI and SOI. The most significant correlations were, overall, found at multi-annual time scales (>7 years). Results help to better understand the current hydroclimatic changes (Megadrought) in a long-term context.

KEYWORDS

Chile, megadrought, SPEI, tree-ring

1 | INTRODUCTION

Hydroclimatic variability is one of the main features of environmental and socio-economic risks due to its potential hazardous impacts on ecosystems and communities (Veldkamp *et al.*, 2006; Kiem and Verdon-Kidd, 2013). An accurate understanding of its origins and causes is still a major challenge in scientific research due to the lack of long-term climatic data (Wilhite and Glantz, 1985; Cook *et al.*, 2016), especially in South America (Garreaud *et al.*, 2009). In Chile the risks associated with hydroclimatic extremes have been demonstrated to be of paramount importance; such as those related to droughts: wildfires (González *et al.*, 2018; Sarricolea *et al.*, 2020), loss of water resources (Olmstead, 2010), reduction of glacier mass (Barcaza *et al.*, 2017), or even fostering of social conflicts in low precipitation areas where the water is commodified (Prieto, 2016). Likewise, extremely wet conditions represent a threat when occurring unexpectedly (Rondanelli *et al.*, 2019).

Considering a scenario of increasing temperatures, higher water demand and a prolonged water shortage, this region will become a high-risk area under any climate change scenario (Bozkurt *et al.*, 2018). Recent climate trends already point in this direction, as several studies have documented a decrease in precipitation (Vuille and Milana, 2007; Escobedo and Sarricolea, 2017; Boisier *et al.*, 2018) and an increase in temperature (Burger *et al.*, 2018; Stolpe and Undurraga, 2016; Meseguer-Ruiz *et al.*, 2018) since the mid-20th century.

From 2010 to 2018, central Chile suffered an intense drought, the so-called “Megadrought” (MD), with precipitation dropping to 45% below average (Garreaud *et al.*, 2020) and coinciding with the warmest years of the last decades (Pitaric, 2018). A precise contextualization of this and other extreme events in the instrumental period has already been presented in previous studies (e.g., Sarricolea and Meseguer-Ruiz, 2015; Aldunce *et al.*, 2017; Garreaud *et al.*, 2017, 2020). Although these investigations drew a detailed picture of the hydroclimatic trends over the last decades in central Chile, the long-term context can only be addressed using proxy records. Tree-ring growth analysis can provide such a long-term perspective of the climatic variability without sacrificing the advantages of instrumental data such as temporal resolution or regional representativeness. *Austrocedrus chilensis* is a relatively abundant, drought-sensitive conifer from the Andean region that can live for more than 1,000 years (Christie *et al.*, 2011), which makes it a suitable species for climate reconstruction based on proxy data. This species has been widely used to reconstruct past climatic variability in central Chile, especially precipitation (LaMarche, 1978; Boninsegna, 1998;

Le Quesne, 2006; Le Quesne *et al.*, 2009) but also droughts (Christie *et al.*, 2011).

Most of these studies focused on the austral winter–early summer season (June to December), trying to reproduce the past fluctuations of water inputs and to identify significant extreme dry and wet periods. However, the use of absolute (or *z*-scores) precipitation values avoids the multiscalar-dimension aspect of drought. It is well known that the response to drought varies between the different components of the hydrologic system (i.e., atmospheric boundary-layer, soil, river flows, reservoirs) during (and after) an extreme hydroclimatic period. If the aim is determining extremes, the consideration of cumulative time scales rather than instantaneous values in water deficit or excess allows for a differentiation between the thresholds characterizing each component of the system. Therefore, this approach is useful for the hydroclimatic evaluation of natural ecosystems (e.g., hydrological modelling, habitat evolution) and socioeconomic development (e.g., crops or water resources) (Vicente-Serrano *et al.*, 2010). The Standardized Precipitation Index (SPI) (McKee *et al.*, 1993) provides a solution taking into account all these preconditions, but it is only based on rainfall, assuming stationarity in the rest of the climatic variables (i.e., temperature, like all other climatic variables, is considered to remain constant, without a temporal trend). This assumption is no longer valid in the current warming scenario. The hydroclimatic extremes are a combination of a lack/excess of water and its atmospheric demand over time, and both parameters can be quantified through the calculation of the water balance based on evapotranspiration, thereby considering other variables besides just precipitation. The Standardized Precipitation Evapotranspiration Index (SPEI) is based on the SPI but solves the temperature-stationarity problem by including temperature as a complementary variable to compute the potential evapotranspiration (Vicente-Serrano *et al.*, 2010). While several SPEI long-term reconstructions using tree-rings as proxy have been developed in different parts of the world (e.g., Seftigen *et al.*, 2015; Zhao *et al.*, 2017; Bhandari *et al.*, 2019), none of them have targeted the SPEI for reconstruction over South America.

The longest climatic reconstruction in the region, based on *A. chilensis*, was developed by Garreaud *et al.* (2017), extending back to the year 1000 CE in a June–December precipitation reconstruction, being one of the few millennium-long tree-ring based hydroclimate reconstructions in the world (Ljungqvist *et al.*, 2019). Furthermore, Christie *et al.* (2011) reconstructed a drought index (PDSI) from 1346 to 2002 CE, as a major breakthrough in long-term hydroclimate research in central

Chile. Although they identified several past extreme drought events, the PDSI has a fixed temporal scale, limiting the ability to identify mid- to low-frequency events that depend on the cumulative history of hydroclimatic variability.

In this work, we aim to identify and analyse the extreme hydroclimatic events that occurred in central Chile since the 16th century by reconstructing the SPEI using a long tree-ring chronology. The analysis is not constrained to dry periods, which are undoubtedly of great interest in this part of the world, but also includes wet periods, as they allow putting the magnitude of the events in a long-term context. In a first stage, we use instrumental temperature and precipitation data from the city of Santiago spanning a period of 79 years (1938–2016) and existing (and updated) tree-ring series from an Andean area near Santiago (Cajón del Maipo), to reconstruct the SPEI from 1536 to 2016. In a

second stage, we explore the relationship between the temporal fluctuations of the SPEI and several teleconnection indices.

2 | STUDY AREA, DATA SETS AND METHODOLOGICAL APPROACH

The research is focused on central Chile (30–38°S) (Figure 1). The area is strongly affected by the South Pacific anticyclone (SPA) and the El Niño – Southern Oscillation (ENSO), both of them modulating, along with winter subpolar lows, a Mediterranean climate with distinctly seasonal precipitation. Moreover, Boisier *et al.* (2016) state that climate change has modified atmospheric circulation patterns, especially subtropical high-pressure systems moving to higher latitudes, which directly influences the intensity of droughts affecting

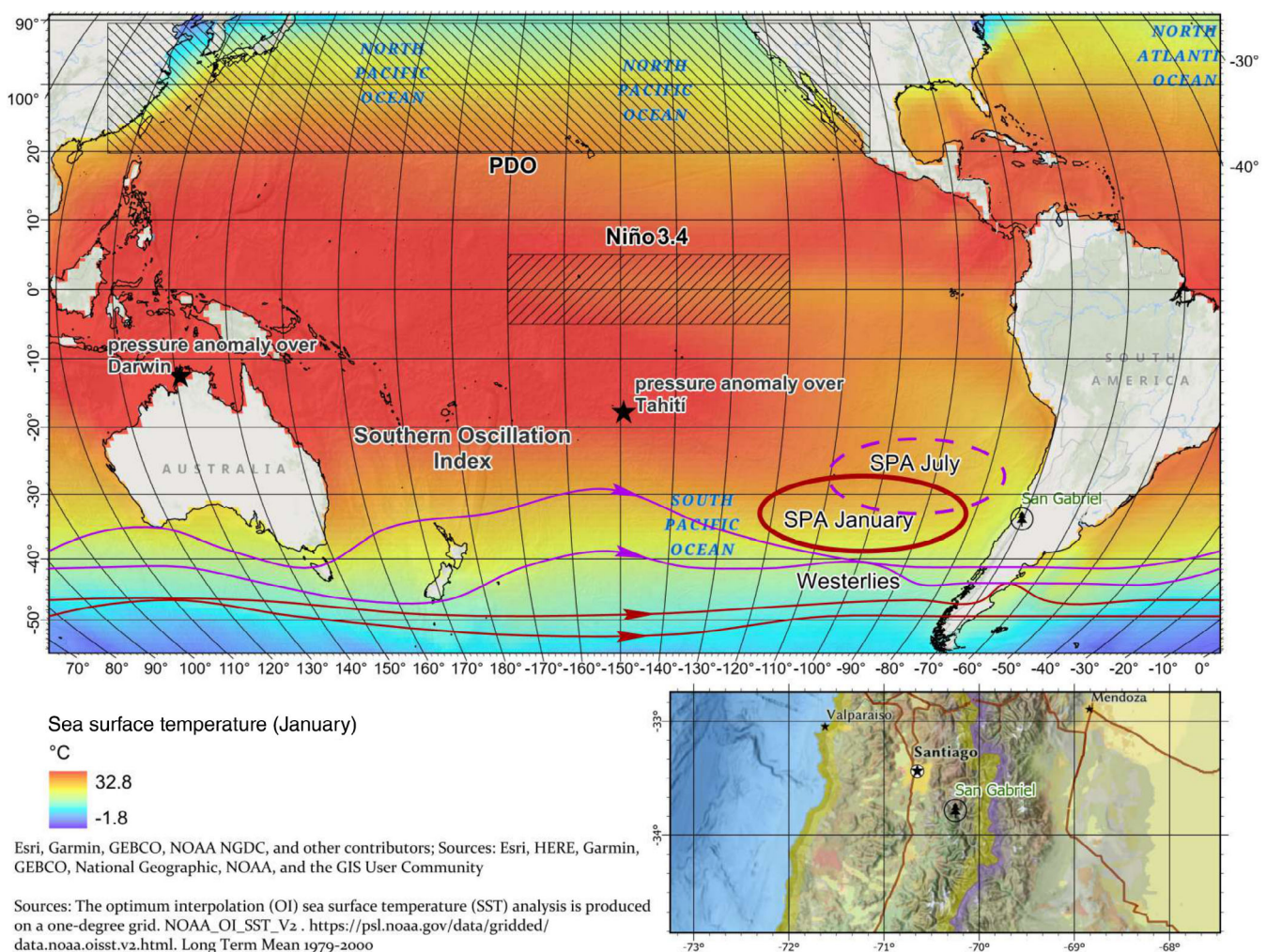


FIGURE 1 Main climate modes affecting the study area and location of the observatory of Quinta Normal (Santiago) and tree-ring chronologies (San Gabriel) [Colour figure can be viewed at wileyonlinelibrary.com]

central Chile. These climatic characteristics are further modulated by the orography, due to an altitudinal range of more than 3,000 m across less than 100 km from the Pacific coastline to the summits of the Andes. It has been shown that modes of interannual to multi-decadal variability (such as the Pacific Decadal Oscillation [PDO], and ENSO) explain a large fraction of south-central Chile rainfall (Quintana and Aceituno, 2012; Amaro de Lima *et al.*, 2018). These modes also affect low-level atmospheric circulation in this area (Sarricolea *et al.*, 2018) and the occurrence of extreme events (Erfanian *et al.*, 2017).

2.1 | Instrumental records

We used monthly precipitation and temperature data from the “Quinta Normal” observatory, managed by the Dirección Meteorológica de Chile (DMC) and located in Santiago (Figure 1). It represents the longest-standing instrumental precipitation record in the Southern Hemisphere with observations beginning in 1867. Climatic analyses (Aceituno *et al.*, 2008; González-Reyes, 2016) show a negative precipitation trend from the end of 19th century to present-day (Quintana and Aceituno, 2012). Temperature recordings at the same observatory started in 1861, but the series has long periods of missing and suspect values between 1876 and 1937. Since 1938, data are continuous and available from the yearbooks of the DMC, digitized by the NOAA Central Library Data Imaging Project (<https://library.noaa.gov/Collections/Digital-Docs/Foreign-Climate-Data/Chilean-Climate-Data>). We did not apply any specific quality control to the dataset since the quality of the observatory has been verified in several previous reconstructions (Bonisejna, 1998; Le Quesne *et al.*, 2009; González-Reyes, 2016).

We used these precipitation and temperature series to compute the monthly SPEI at lags from 1 to 15 months using the R package SPEI (Beguería and Vicente-Serrano, 2017). The Thornthwaite method (Thornthwaite, 1948) was used to calculate the potential evapotranspiration. The SPEI value involves: (a) a lag in months, indicating the number of months considered to assess the hydroclimatic situation, and (b) a month of the year when the lag ends. For example, a $\text{SPEI}_{14_{\text{Aug}}}$ value represents the hydroclimatic situation of August considering the previous 14 months. When computed over several years, the resulting SPEI series will show the hydroclimatic situation of each August with respect to the 14 prior months. Details on SPEI are widely described in Vicente-Serrano *et al.* (2010).

2.2 | Tree-ring reconstruction

2.2.1 | Data collection

To develop the tree-ring chronology, we took advantage of the existing tree-ring growth series of *A. chilensis* in the “Cajon del Maipo” area near San Gabriel (Figure 1), located ~50 km southeast of Santiago. These data were collected by LaMarche *et al.* (1979) and stored in the International Tree-Ring Databank (Grissino-Mayer and Fritts, 1997). The information contained in the dataset includes 61 tree-ring growth series extending back from 1131 to 1976 CE. Here we aimed to update this dataset in order to capture the current period of warming. Therefore, in January 2017, we collected 28 additional samples from 16 trees (i.e., the outermost ring is 2016) of *A. chilensis* growing in the same region. These trees take advantage of the available soil and are located on a steep south-facing slope between 1,300 and 1,600 m a.s.l. (Figure 2). This species is well adapted to growing at higher elevation, including isolated slopes, which favours the presence of old specimens. As shown by Le Quesne *et al.* (2009) it is particularly sensitive to hydroclimatic variability.

Next, the core samples were processed according to standard procedures (Stokes and Smiley, 1968). Each sample was scanned to identify and date the exact position of the annual rings, and the image software CoRecorder 8.1 (Larsson, 2012) was used to objectively define the exact position of the transition between annual rings. Finally, the tree-ring width was measured separately at 0.01 mm precision using a LINTAB table (Rinn, 2005), and cross dating was verified using the COFECHA software (Holmes, 1983).

2.2.2 | Chronology development

To develop the tree-ring reconstruction we combined the existing 61 raw tree-ring width series with the 28 newly collected series. To preserve the inter-annual to multi-decadal scale variability and to eliminate the age-related trend in the radial growth, we standardized the individual 89 tree-ring width series using the *dplR* standardization package (Bunn, 2008). Each ring-width series was fitted with a 100-year smoothing spline to retain not only the high-frequency variability, but especially the mid-to-low frequency variability.

We then assembled the individual standard series to develop the regional tree-ring width index chronology (TRI) using a robust mean estimation. Finally, the chronology confidence-interval was estimated using running

FIGURE 2 Sampling site at San Gabriel (central Chile). *A. chilensis* has a sparse distribution all along the slope (a). Two sample cores extracted in 2017 campaign of 235 (b) and 302 (c) years [Colour figure can be viewed at wileyonlinelibrary.com]



inter-series correlations (R_{bar}) and the express population signal (EPS) metric (Wigley *et al.*, 1984). EPS provides an estimate of the match between mean chronology based on a finite number of trees and its hypothetically perfect chronology (Cook *et al.*, 1990). Values equal to or above 0.85 are considered to ensure that a chronology is suitable for climate reconstruction (Wigley *et al.*, 1984).

2.2.3 | Climate–growth relationship and climate reconstruction

We calibrated the TRI chronology against the SPEI with a lag from 1 to 15 months using the station-based climate data of Santiago as done in previous studies to reconstruct the SPEI (Ma *et al.*, 2015; Tejedor *et al.*, 2017). This calibration consisted of the correlation between the TRI and each of the SPEI series from January to December at lags from 1 to 15 months during the instrumental period (1938–2016). The best correlated series of SPEI was selected as target for reconstruction.

Then, to evaluate the accuracy of the model used for climate reconstruction, we split the dataset into two equally long periods for calibration and verification (Fritts, 1976). These periods were 1938–1977 and 1978–2016. We tested the consistency of the linear model using the Pearson's correlation coefficient (r), a 30-year moving correlation, the reduction of error (RE) and sign test. RE provides a highly sensitive measure of reliability of a reconstruction (Akkemik *et al.*, 2005), ranging from +1, meaning perfect agreement, to minus infinity. In general, positive RE values are interpreted as a reconstruction showing some skill (Fritts *et al.*, 1990). The sign test compares the number of agreeing and disagreeing interval trends, from year to year, between the observed and

reconstructed series (Čufar *et al.*, 2008). Finally, we transferred the chronology into a climate reconstruction using a linear regression model (using the full 1938–2016 period). To identify and evaluate extreme events, we selected values of the reconstructed series exceeding the SPEI value of $\pm 2\sigma$ as indicated by McKee *et al.* (1993), who chose that threshold to identify a severe event occurrence. While all thresholds regarding the identification of extreme events are arbitrary, previous studies in different climates used values close to $\pm 2\sigma$ (e.g., Bachmair *et al.*, 2015, 2016; Danandeh Mehr and Vaheddoost, 2020).

2.3 | Assessment of potential drivers

To assess potential drivers of hydroclimatic variability (SPEI), we analysed the relationship between the SPEI and three regional sea surface temperature (SST)- and sea level pressure (SLP)-based indices from the Pacific Ocean, obtained from the National Oceanic and Atmospheric Administration (NOAA) – National Centers for Environmental Information (NCEI), the NOAA – Earth System Research Laboratories (ESRL), and the NOAA – Climate Prediction Center (CPC): (a) The Pacific Decadal Oscillation (PDO), representing large-scale (multi-) decadal variations of Pacific SST and SLP fields and significantly affecting South American climate (Garreaud *et al.*, 2009; Flantua *et al.*, 2016) with temporal scales of variability ranging from 15–25 to 50–70 years (Mantua and Hare, 2002); (b) The Southern Oscillation Index (SOI), which is based on the difference between western and eastern tropical Pacific SLP and is highly correlated with eastern tropical Pacific SST; and (c) The Niño3.4 index (Trenberth, 1997), describing interannual

variability in central tropical Pacific SST (5°N–5°S, 120°–170°W), and responsible for a significant fraction of inter-annual wintertime precipitation variability in central Chile (Montecinos and Aceituno, 2003).

The three indices were correlated with the reconstructed SPEI at the fixed temporal scale and month chosen by the reconstruction process (14-month lag, using the month of August, see Section 3.1) during their overlapping periods (Table 1). With the aim of evaluating the strength of each teleconnection between modes of SST/SLP variability and the SPEI during different months and cumulative time periods, we computed, from January to December and for all years, the centred moving averages of the indices over cumulative periods (scales) of 1 (non-averaged) to 27 years (every 2 years) as expressed in Equation (1):

$$MA_ind_{m,n,i} = \frac{1}{n} \sum_{k=i-((n-1)/2)}^{i+((n-1)/2)} ind_{m,k}, \quad (1)$$

where, given an annual series of values (*ind*) of an index (PDO, SOI, or Niño3.4) subsetted for a given month (*m*), the value of the moving average (*MA_ind_{m,n,i}*) of a given year *i* depends on the centred average of the values within the fixed window of size *n*. The resulting series for the three indices (*MA_ind_{m,n}*) were correlated with the corresponding averaged reconstructed (*sp_rec_n*) SPEI:

TABLE 1 Overlapping periods and number of overlapping years (in brackets) between modes of SST/SLP variability and the reconstructed SPEI

Index	Overlapping period
PDO	1854–2016 (163)
SOI	1951–2016 (66)
Niño3.4	1870–2016 (147)

$$\rho_{X,Y_{m,n}} = \frac{\sigma_{X_{m,n}Y_n}}{\sigma_{X_{m,n}}\sigma_{Y_n}}, \quad (2)$$

where $\rho_{X,Y}$ is the Pearson correlation between $X_{m,n}$, the averaged index (*MA_ind_{m,n}*) at scale *n* and month *m*, and Y_n , the averaged reconstructed SPEI (*sp_rec_n*) at the same scale *n*. $\sigma_{X_{m,n}Y_n}$ is the covariance between the two variables, and $\sigma_{X_{m,n}}$ and σ_{Y_n} are the SDs of $X_{m,n}$ and Y_n , respectively.

3 | RESULTS

3.1 | SPEI reconstruction

Although the chronology begins in 1131 CE, the analysis was limited to the last 481 years (1536–2016), for which the number of samples was sufficiently high and the EPS (Expressed Population Signal) remained above 0.85 throughout (Figure 3).

For the period 1938 to 2016, the correlations between the chronology and the SPEI, based on the instrumental data at different lags (Figure 4), showed the highest values from July to December, coinciding with the rainy season in winter and spring, and at lags longer than 12 months (SPEI considering, at least, the prior 12 months), which means that the TRI chronology is also influenced by previous year's conditions. Overall, lowest correlations (<0.4) were found at all time scales from January to June (summer and autumn) and throughout the year when fewer than the previous 12 months were considered. Notably, it is evident that the hydroclimatic conditions during the prior 6 months barely affect the TRI (most of the correlations are non-significant – blank cells – or very low – below 0.4). The highest correlation (0.56) occurred in August at a time scale of 14 months (SPEI14_{Aug}). The SPEI at this timescale is useful to explain the tree-growth response to droughts considering a complete hydrological year.

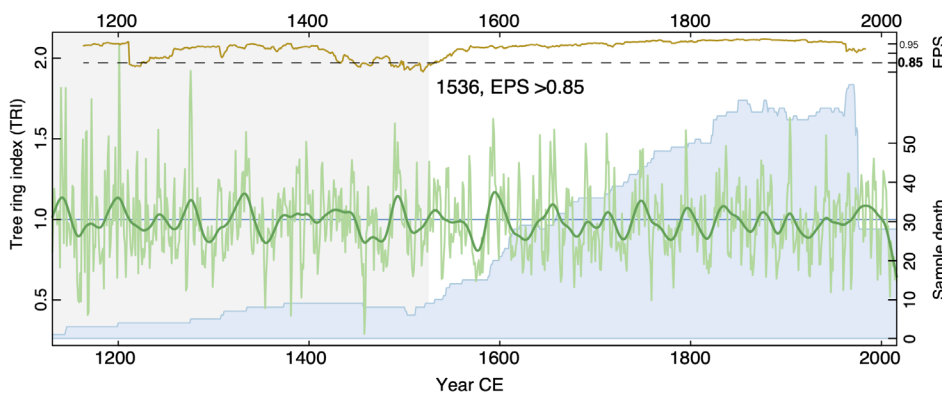


FIGURE 3 Tree ring index (thin green line) and its 50-year moving average (bold smooth green line), number of samples (light blue shading) and EPS surpassing threshold in 1536 [Colour figure can be viewed at wileyonlinelibrary.com]

FIGURE 4 Upper panel: Walter-Lieth diagram showing wet (blue area) and dry (yellow area) seasons, monthly precipitation (blue line) and temperature (red line). Lower panel: correlation matrix between the monthly (X axis) SPEI at lags from 1 to 15 months (Y axis) and the regional chronology over the period 1938–2016. Only Pearson correlation values at the $\alpha = .05$ significance level are shown. Highest correlation, at August-14 months is highlighted with black box [Colour figure can be viewed at wileyonlinelibrary.com]

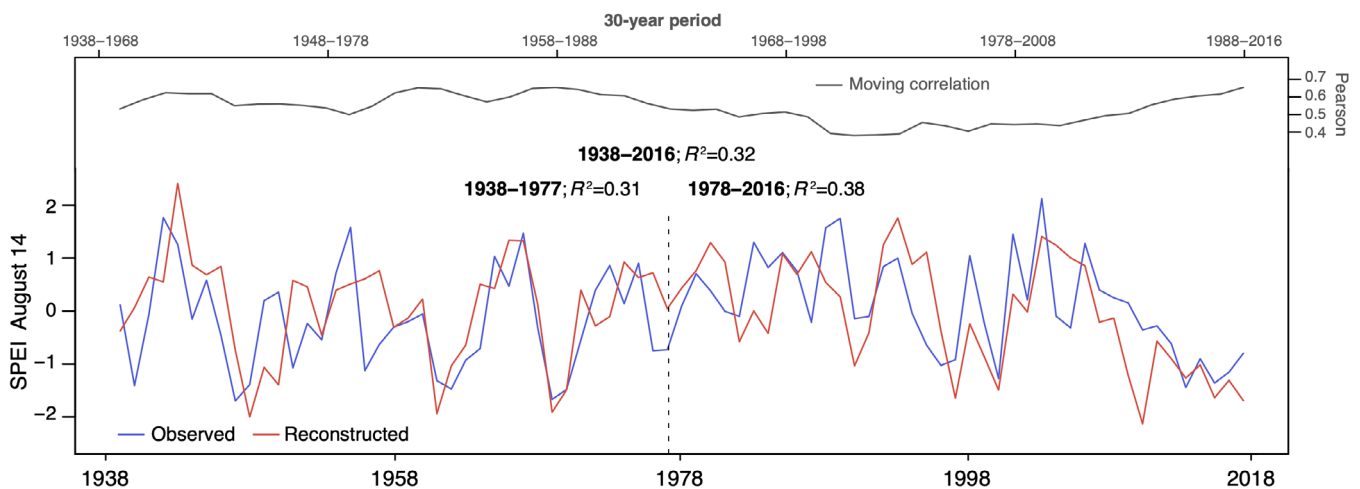
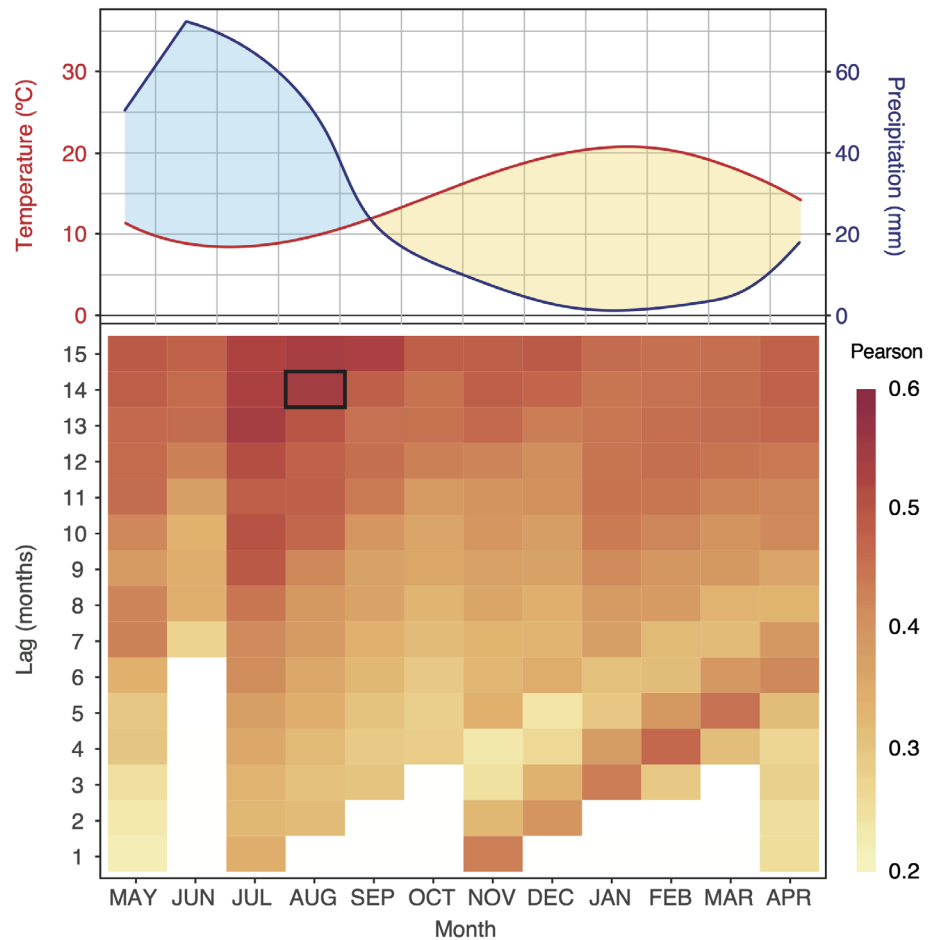


FIGURE 5 Calibration and verification results of the SPEI₁₄_{Aug} reconstruction in the instrumental period [Colour figure can be viewed at wileyonlinelibrary.com]

The two models obtained for the calibration and verification periods 1938–1977 and 1978–2016 (Figure 5), reached R^2 values of 0.31 and 0.38, respectively (Table 2). These differences between the calibration

periods are due to the high variability in the TRI chronology that cannot be explained with climatic parameters alone. However, the 30-year moving correlation between observed and reconstructed SPEI varied from

TABLE 2 Calibration and verification statistics of the SPEI14_{Aug} reconstruction in the instrumental period

Period	Years	R	R ²	RE	D
Calibration	1938–1977	0.56	0.31	0.33	20+/19–
Verification	1978–2016	0.62	0.38	0.21	29+/16–
Full	1938–2016	0.57	0.32	0.28	49+/30–

Abbreviations: Years, Period used for the calibration/verification reconstruction; R, Pearson correlation coefficient; R², coefficient of determination; RE, reduction of error; D, sign test.

0.45 to 0.70 in the full period, with highest values between 1940 and 1975. We used the full period (1938–2016) for the final linear model to fit the reconstruction to the full instrumental data series and reconstructed the SPEI14_{Aug} starting in 1536:

$$\text{SPEI14}_{\text{Aug}} = 2.3898 \times \text{TRI}_{\text{res}} - 2.3920 (R^2 = 0.32; p < .01), \quad (3)$$

3.2 | Hydroclimatic variability in central Chile

The reconstruction of the SPEI shows that 2 out of the 3 driest years (Figure 6a and Table 3) since the 16th century occurred since 1947 (1947 and 2009). The years identified as extremely wet, on the other hand, were more equally distributed across time, but none have occurred since the start of the second half of the 20th Century. When averaging the reconstruction with an 11-year moving window (Figure 6b) to emphasize lower-frequency variance in the reconstruction, cyclic fluctuations were revealed until the end of the 19th century, while the 20th century is characterized by a dry period at the beginning, followed by muted variability, and then a long wet period, ending with the strong drought of the early 21st century. Overall the smoothed (11-year time scale) SPEI14_{Aug} shows a change in the temporal distribution of the extreme events with the most intense and long wet

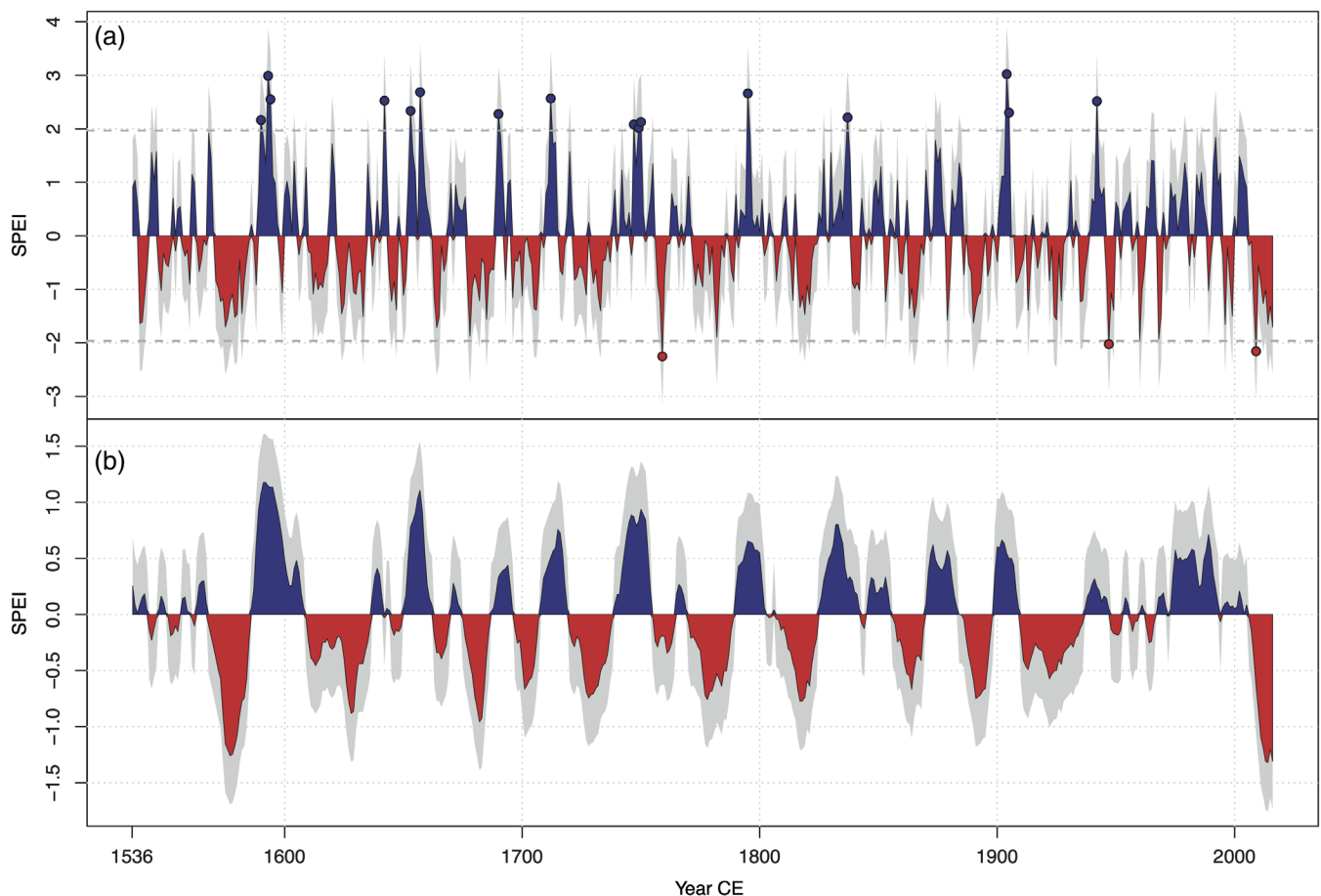


FIGURE 6 SPEI14_{Aug} reconstruction since 1536 CE for Central Chile. (a), Annual values of negative (red) and positive (blue) anomalies. Grey shading indicates the RMSE of the residuals. The wettest (blue points) and driest (red points) years exceeding the threshold of SPEI ± 2 (dashed bold grey line) are shown. (b) Same as (a) but aggregated at an 11-year moving average [Colour figure can be viewed at wileyonlinelibrary.com]

TABLE 3 The most extreme dry and wet years

Century	Wet extreme years	Dry extreme years
16th	1590 (+2.16) 1593 (+2.99) 1594 (+2.55)	
17th	1642 (+2.53) 1653 (+2.33) 1657 (+2.68) 1690 (+2.28)	
18th	1712 (+2.57) 1747 (+2.08) 1749 (+2.02) 1750 (+2.13) 1795 (+2.66)	1759 (−2.25)
19th	1837 (+2.21)	
20th	1904 (+3.02) 1905 (+2.30) 1942 (+2.51)	1947 (−2.02)
21st		2009 (−2.16)

Note: Only years with SPEI exceeding the threshold of ± 2 , based on the SPEI14_{Aug} reconstruction, are shown. Listed by date of occurrence.

period occurring in the first half of the series (1586–1608). The extreme events progressively decrease in intensity until the end of 20th century. Two extreme dry periods were identified; the longer one (1568–1585)

occurred just before the previously noted wet event, and the shorter but more intense period occurs at the end of the series (2006–2016).

3.3 | Relationship between hydroclimatic variability and climate indices

The PDO (Figure 7 left) shows a positive correlation with the reconstruction, especially from January to March and from August to October, with the highest correlation obtained in March (+0.47) when averaged over 13 years. The higher correlations at the 9–27-year time scales are likely due to the low interannual variability of the reconstruction and, therefore, they are the best representation of low-frequency variability.

Conversely, the SOI (Figure 7 centre) shows negative correlations in all months (except May, when no significant values were found) with most negative values in December at time scales from 7 to 27 years (R -values ranging from -0.67 to -0.85). The Niño3.4 index (Figure 7 right) is positively correlated with the SPEI in all months, although correlations are not significant at 1-year time scale and only 1 month (August) is at the 3-year time scale. The highest correlations were found from January to March at 9 to 11-year time scales (highest value in March 11-year: 0.34).

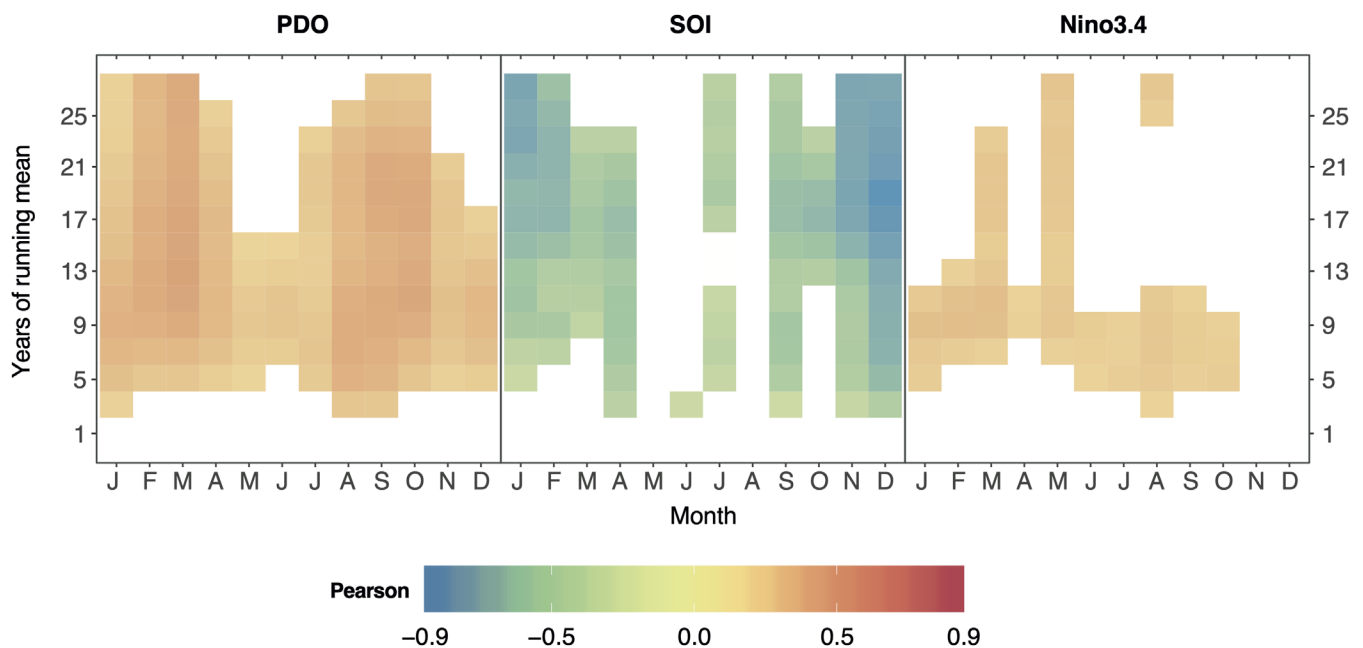


FIGURE 7 Correlation between the three indices of climate variability (PDO, Pacific decadal oscillation; SOI, Southern Oscillation Index and Niño3.4) and the reconstructed SPEI14_{Aug}. The correlations were computed by months (X axis) and moving average windows (Y axis). Only Pearson correlation values at the $\alpha < .01$ significance level are shown [Colour figure can be viewed at wileyonlinelibrary.com]

4 | DISCUSSION

4.1 | SPEI reconstruction challenges

Paleoclimatic reconstructions are of key importance in areas such as South America, where instrumental information is scarce before the 20th century (Garreaud *et al.*, 2009). Here we use 89 tree-ring width series, calibrated with instrumental data, to create a 481-year SPEI reconstruction from the 16th century to present-day (1536–2016 CE) focused on Santiago (Chile). In a previous hydroclimatic reconstruction for central Chile, Christie *et al.* (2011) used pre-whitened tree-ring chronologies to reconstruct the PDSI, calibrated with 40 years of instrumental data (1960–2000 AD) to capture the high-frequency signal. While such a procedure allows correctly identifying interannual variability, it does not reproduce the mid- to low-frequency fluctuations and thus complicates the analysis of prolonged droughts in a long-term context (such as the 2010–2015 MD). We opted to retain the mid-to-low frequency variability, as done in previous reconstructions (e.g., Le Quesne *et al.*, 2009; Masiokas *et al.*, 2012; Garreaud *et al.*, 2017), since pre-whitened time series will generally not carry important stochastic properties embedded in respective original time series resulting from persistence and seasonality, and thus cannot preserve the structure of variability across time scales (Razavi and Vogel, 2018). Boucher *et al.* (2011) improved this low-frequency hydroclimatic evolution by merging different proxies, but they also used the PDSI (with the same limitations) and constrained to the austral summer (DJF). Our reconstruction, therefore, is the first in Chile that is based on a drought index that considers the multiscale character of precipitation. This represents a significant breakthrough due to the consideration of the large-scale (both in time and magnitude) and the cumulative characteristics of hydroclimatic events through time, which is essential to evaluate the duration, intensity and frequency of extreme events. In this regard, the SPEI allows for the identification of wet and dry events at different cumulative temporal scales, including, but not limited to, extreme ones. However, the long-term contextualization using the reconstructed series greatly helps to identify those events, in terms of duration and/or magnitude, that stand out from the regular behaviour. The SPEI provides a more accurate characterization of magnitude and duration of the events due to its multi-scale nature along with its ability to be computed at different time scales (lag).

Although our reconstruction has uncertainties (R^2 of 0.32 between observations and reconstruction in the 1938–2016 period) and thus must be interpreted with caution, the results provide a substantial improvement in

the understanding of the hydroclimatic variability in the Santiago region in central Chile. The existing chronology is longer than our final reconstruction; however, due to limited replication prior to 1536 CE, we selected the 1536–2016 CE period for the reconstruction, as more tree samples are available and the EPS remained continuously above the commonly established threshold (0.85) (Figure 3). An extended and more robust reconstruction could be developed by: (a) increasing the replication of long tree-ring width series; and (b) constraining the calibration period to the more recent decades. Despite the limitations and potential uncertainties, we used a more extended instrumental period to calibrate the reconstruction because the use of a shorter period assumes that the calibration depends on a climatic period with specific characteristics (e.g., wetter or drier), which are different from the known climate data. The use of long data series allows embracing a wider envelope of climate variability that should be reflected in the reconstruction.

4.2 | A reconstruction of long-term hydroclimatic variability

The reconstructed SPEI represents a useful tool to evaluate the long-term evolution of hydroclimatic events in central Chile. We found that at the beginning of the 21st century this region experienced the most intense drought of the past 481 years. This event, already described in Garreaud *et al.* (2017, 2020), was associated with significant ecological and socioeconomic impacts over the territory. Throughout the period analysed, the duration and intensity of dry and wet events becomes progressively more muted, especially during the mid-20th century, a phenomenon already documented (Le Quesne, 2006) and also reflected in streamflow reconstructions (Fernández *et al.*, 2018). When analysing hydroclimate signals at the 11-year scale, however, this tendency disappears after the mid- 20th century, being replaced by two subsequent prolonged events of positive and negative anomalies, respectively. Over the instrumental period the reconstruction is consistent with previous research, considering that prior studies did not analyse the same time scale and month of our SPEI reconstruction. For instance, Garreaud *et al.* (2017) (1916–2015 period) showed a $SPI_{12_{Dec}}$ with driest years from 2010 to 2015 and Spinioni *et al.* (2019) found a similar pattern in Argentina (1951–2016) at time scales of 12 and 24 months. Saurral *et al.* (2017) observed a marked decrease of annual precipitation starting at the beginning of the 20th century.

The general evolution of the hydroclimatic events over the full reconstruction period (1536–2016) is similar to the one found in the 1346–2000 CE PDSI

reconstruction of Christie *et al.* (2011). Despite the differences in the thresholds considered, there is a good correspondence between the number of extreme dry and wet events, although not in the years, which likely can be attributed to different methods used for calculating both indices and to the cumulative temporal scale of the SPEI. For example, the 18th century in both reconstructions shares one dry and four wet events, as well as the late wet events in the 16th century. The 20th century is similar in both series, with slightly more extreme events detected in their reconstruction.

The SPEI reconstruction is also consistent with the 655-year streamflow reconstruction of the Neuquén river (Argentina) made by Mundo *et al.* (2012) using tree rings from *Araucaria araucana* and *A. chilensis* to identify dry and wet events in the 1346–2000 period. SPEI14_{Aug} detected most of the noticed droughts in that study, such as the 1968 drought (SPEI of -1.93) described in Prieto *et al.* (2010), the 1998–1999 strong La Niña conditions (-1.50 in 1999) and the 1924 (-1.50) record of lowest precipitation in Santiago (Rutllant and Fuenzalida, 1991).

Furthermore, Vicuña-Mackenna (1877) already described the first well-documented drought during 1637–1640, detected in our reconstruction at the 11-year scale (Figure 6b) as one of the longest ones (not extreme),

followed by an extreme wet episode (1642: SPEI of $+2.53$). Jana *et al.* (2019) described many other drought periods in central Chile extracted from the work of Vicuña-Mackenna, especially in the 16th and 17th centuries that were not detected in our reconstruction, probably due to the 14-month scale of the SPEI. Some other events reported in that work, however, were detected considering this lag (e.g., the 1748 CE flood in Santiago is reflected with SPEI values of $+2.08$, $+2.02$ and $+2.13$ in 1747, 1749 and 1750, respectively). Overall, if we lowered the threshold value of $\pm 2\sigma$, probably most of the extreme hydroclimatic events identified in Jana *et al.* (2019) could also be detected in our reconstruction (Table 4).

4.3 | Climatic indices as potential drivers of SPEI

The hydroclimate of the Santiago region is influenced on seasonal to decadal timescales by changes in the large-scale circulation, which in turn is being modulated by the main modes of Pacific SST and SLP variability. Several studies have addressed these relationships to analyse droughts (Boucher *et al.*, 2011; Christie *et al.*, 2011; Meza, 2013; Zambrano *et al.*, 2018), temperature (Burger

TABLE 4 Dry and wet events documented in previous works and detected by SPEI14_{Aug}

Dry events	Wet events	Source	Reconstructed variable
1633; 1781–1782; 1863; 1892; 1904 ; 1924; 1942 ; 1949; 1968; 1999*	1884; 1931*; 1965; 1992	Le Quesne (2006)	June–December precipitation
1682; 1818; 1819; 1821; 1913; 1996; 1999*	1609; 1635; 1870	Lara <i>et al.</i> (2008)	December–May streamflow
1924; 1942	1653 ; 1851	Le Quesne <i>et al.</i> (2009)	Annual precipitation
1913; 1924; 1949; 1999*	1849; 1965*; 1986; 1991;	Christie <i>et al.</i> (2011)	December PDSI
1625; 1633; 1682; 1685; 1817–1819; 1821; 1924; 1968–1969; 1999*	1590–1594 ; 1653–1655 ; 1657–1658 ; 1720; 1942 ; 1979; 1984	Urrutia <i>et al.</i> (2011)	April–March streamflow
1573–1580; 1624–1625; 1629–1630; 1633; 1678; 1682; 1685	1590–1593 ; 1594–1596 ; 1653–1655 ; 1657–1658 ; 1849; 1851; 1858	Masiokas <i>et al.</i> (2012)	Snowpack
	1837–1838 ; 1876	Morales <i>et al.</i> (2012)	November–October precipitation
1924; 1968; 1969; 1996; 2012–2016		Garreaud <i>et al.</i> (2017)	June–December precipitation
1577; 1705; 1781; 1782; 1863	1537*; 1544; 1609; 1747* ; 1748– 1749* ; 1770; 1836; 1837 ; 1851*; 1858	Vicuña-Mackenna (1877), compiled by Jana <i>et al.</i> (2019)	Single events

Note: Some events are detected in the following year (emphasized with an asterisk). Only events with SPEI higher than 1 or lower than -1 are shown. Bold years indicate SPEI exceeding 2 or -2 .

et al., 2018) and precipitation changes (Rutllant and Fuenzalida, 1991; Vuille and Milana, 2007; Morales *et al.*, 2012; González-Reyes *et al.*, 2017; Boisier *et al.*, 2016; 2018), amongst others. While some of these previous studies were focused on ocean–atmosphere forcings, our analysis only includes a first attempt at evaluating potential drivers of the reconstructed hydroclimatic variability.

The SPEI reconstruction is positively correlated with the PDO, meaning that warm (cool) phases of the PDO are associated with wet (dry) conditions in central Chile, consistent with previous studies (González-Reyes *et al.*, 2017; Valdés-Pineda *et al.*, 2018) and with other regions (Fang *et al.*, 2014). This relationship is likely strengthened by the fact that both PDO and the SPEI14_{Aug} emphasize mid- to low-frequency variability on multiannual to decadal timescales. The SOI is negatively correlated with the SPEI14_{Aug}, again consistent with the expectations, given that the Southeast Pacific Subtropical Anticyclone is significantly weakened during the negative phase of the Southern Oscillation, thereby enhancing precipitation in central Chile (Rutllant and Fuenzalida, 1991). We noted the strongest relationship occurring in December at the 11-year timescale, despite the strong interannual character of the SOI.

The Niño3.4 index is highly anti-correlated with the SOI; hence it comes as no surprise that it is positively correlated with the SPEI index, consistent with abundant literature on the ENSO hydroclimate influence in central Chile (e.g., Montecinos and Aceituno, 2003; Erfanian *et al.*, 2017; Amaro de Lima *et al.*, 2018). However, slightly higher correlations in all months were expected. The relatively weak correlation observed between the reconstruction and the index may partly be explained by the biennial tendency of ENSO to switch from its positive to its negative phase (and vice versa) within the 14-month timescale of the studied SPEI. Hence the Niño3.4 index does not really explain prolonged drought conditions in central Chile, such as those represented by the SPEI14_{Aug}. Indeed, Garreaud *et al.* (2017, 2020) found ENSO-neutral conditions along the duration of the MD (2010–2015) and Vuille and Milana (2007) pointed out that the long-term 20th century trend toward increasing aridity is not related to ENSO. Valdés-Pineda *et al.* (2016) showed that there is a higher probability (10–30%) of very wet conditions in central Chile during El Niño years.

5 | CONCLUSIONS

We analysed the hydroclimatic variability in central Chile from 1536 to 2016 through the reconstruction of

the SPEI. To do that we used: (a) long available data series (1938–2016) of observed monthly precipitation and temperature at Santiago, Chile; (b) a collection of dendrochronological series extracted from previous research and updated with fieldwork in 2017; and (c) a correlation analysis of the reconstructed SPEI with three climate indices to identify potential large-scale forcing mechanisms of droughts and wet periods.

The SPEI reconstruction (focused on the month of August, with a lag of 14 months), showed that the frequency of extreme wet years was higher in the 17th and 18th centuries (1/2 of all the extreme years occurred in this period) while the extreme droughts were more frequent in the late 20th and early 21st centuries. The middle of the 20th century represented the breakpoint for the hydroclimatic history, when: (a) the interannual variability increased; (b) the wet events became less intense (none of them identified as extreme); (c) the dry extreme events became more frequent; and (d) the most intense dry event was found (starting in 2009), coinciding with the so-called Megadrought.

The correlation analysis between the SPEI14_{Aug} and the climate indices showed overall positive correlations with PDO and Niño3.4, both being significant when aggregating them at time scales from 3 to 11 years. The strongest correlations were found in austral summer (DJF) for both ENSO and PDO and in winter for the PDO. Conversely, negative correlations were found between the SPEI14_{Aug} and the SOI in all months, especially in December and when aggregating the data over longer timescales (7–27 years). Our analysis shows that Pacific SST and SLP variations, especially at multiannual timescales (>7 years) significantly affected past hydroclimatic variability over central Chile. However, the relationships documented in this study can be improved by: (a) extending the length of the period of observations, which varies between indices, and (b) reducing the uncertainty of the reconstruction. While the first cannot be controlled, the second aspect could be improved with a better replication of the dendrochronological series. In addition, our understanding of the relationship between the climate indices and the reconstructed SPEI is limited by the nature of the correlation analysis. Further research focused on ocean–atmosphere variability could improve the attribution of potential drivers of the hydroclimatic variability.

Yet, this first SPEI reconstruction from central Chile documents the hydroclimate variability in the region over the last five centuries, showing a change in the variability since the mid-20th century and highlighting the fact that the most recent years represent the most intense sustained drought that this region has experienced throughout the period analysed.

ACKNOWLEDGEMENTS

R. S. N. is funded by a “Juan de la Cierva” postdoctoral grant FJCI-2017-31595. This work was developed under the project CAS/1900020 funded by the Spanish Ministry of Science and the Fulbright Foundation. O. M. R., P. S. and R. S. N. thank the Climatology Group (2017SGR1362, Catalan Government) and the CLICES Project (CGL2017-83866-C3-2-R). R. S. N. and M. D. L. are supported by the Government of Aragón through the “Programme of research groups” (group H38, “Clima, Agua, Cambio Global y Sistemas Naturales”) and thank the project CGL2015-69985-R. E. T. and M. V. were partially supported by NSF-PIRE (OISE-1743738) and NSF-P2C2 (AGS-1702439). M. F. is funded by a postdoctoral grant CONICYT PIA AFB170008 of the Institute of Ecology and Biodiversity (IEB). The authors thank the Dirección Meteorológica de Chile (DMC) for the climatic data and the National Oceanic and Atmospheric Administration (NOAA) for the climatic indices’ series.

ORCID

Roberto Serrano-Notivoli  <https://orcid.org/0000-0001-7663-1202>

Ernesto Tejedor  <https://orcid.org/0000-0001-6825-3870>

Pablo Sarricolea  <https://orcid.org/0000-0002-6679-2798>

Oliver Meseguero-Ruiz  <https://orcid.org/0000-0002-2222-6137>

Mathias Vuille  <https://orcid.org/0000-0002-9736-4518>

Magdalena Fuentealba  <https://orcid.org/0000-0003-2321-6069>

Martín de Luis  <https://orcid.org/0000-0002-7585-3636>

REFERENCES

- Aceituno, P., Prieto, M.D.R., Solari, M.E., Martínez, A., Poveda, G. and Falvey, M. (2008) The 1877-1878 El Niño episode: associated impacts in South America. *Climatic Change*, 92, 389–416. <https://doi.org/10.1007/s10584-008-9470-5>.
- Akkemik, Ü., Da deviren, N. and Aras, A. (2005) A preliminary reconstruction (A.D. 1635–2000) of spring precipitation using oak tree rings in the western Black Sea region of Turkey. *International Journal of Biometeorology*, 49(5), 297–302. <https://doi.org/10.1007/s00484-004-0249-8>.
- Aldunce, P., Araya, D., Sapiain, R., Ramos, I., Lillo, G., Urquiza, A. and Garreaud, R. (2017) Local perception of drought impacts in a changing climate: the mega-drought in Central Chile. *Sustainability*, 9(11), 2053. <https://doi.org/10.3390/su9112053>.
- Amaro de Lima, A., Andreoli, R.V. and Kayano, M.T. (2018) Review: sub-monthly variability of the south American summer precipitation under El Niño and La Niña backgrounds during the 1998–2012 period. *International Journal of Climatology*, 38, 2153–2166. <https://doi.org/10.1002/joc.5430>.
- Bachmair, S., Kohn, I. and Stahl, K. (2015) Exploring the link between drought indicators and impacts. *Natural Hazards and Earth System Science*, 15, 1381–1397. <https://doi.org/10.5194/nhess-15-1381-2015>.
- Bachmair, S., Svensson, C., Hannaford, J., Barker, L.J. and Stahl, K. (2016) A quantitative analysis to objectively appraise drought indicators and model drought impacts. *Hydrology and Earth System Sciences*, 20, 2589–2609. <https://doi.org/10.5194/hess-20-2589-2016>.
- Barcaza, G., Nussbaumer, S.U., Tapia, G., Valdes, J., Garcia, J.L., Videla, Y., Albornoz, A. and Arias, V. (2017) Glacier inventory and recent glacier variations in the Andes of Chile, South America. *Annals of Glaciology*, 57, 166–180. <https://doi.org/10.1017/aog.2017.28>.
- Beguieria, S., Vicente-Serrano, S.M. (2017) SPEI: calculation of the standardised precipitation-evapotranspiration index. R package version 1.7. Available at: <https://CRAN.R-project.org/package=SPEI>.
- Bhandari, S., Gaire, N.P., Shah, S.K., Speer, J.H., Bhujju, D.R. and Thapa, U.K. (2019) A 307-year tree-ring SPEI reconstruction indicates modern drought in western Nepal Himalayas. *Tree-Ring Research*, 75(2), 73–85. <https://doi.org/10.3959/1536-1098-75.2.73>.
- Boisier, J.P., Álvarez-Garretón, C., Cordero, R.R., Damiani, A., Gallardo, L., Garreaud, R., Lambert, F., Ramallo, C., Rojas, M. and Rondanelli, R. (2018) Anthropogenic drying in Central-Southern Chile evidenced by long-term observations and climate model simulations. *Elementa Science of the Anthropocene*, 6(1), 74. <http://doi.org/10.1525/elementa.328>.
- Boisier, J.P., Rondanelli, R., Garreaud, R.D. and Muñoz, F. (2016) Anthropogenic and natural contributions to the Southeast Pacific precipitation decline and recent megadrought in Central Chile. *Geophysical Research Letters*, 43(1), 413–421. <https://doi.org/10.1002/2015GL067265>.
- Boninsegna, J.A. (1998) Santiago de Chile winter rainfall since 1220 as being reconstructed by tree rings. *Quaternary South American Antarctic Peninsula*, 7, 315–326.
- Boucher, E., Guiot, J. and Chapron, E. (2011) A millennial multiproxy reconstruction of summer PDSI for Southern South America. *Climate of the Past*, 7, 957–974. <https://doi.org/10.5194/cp-7-957-2011>.
- Bozkurt, D., Rojas, M., Boisier, J.P. and Valdivieso, J. (2018) Projected hydroclimate changes over Andean basins in Central Chile from downscaled CMIP5 models under the low and high emission scenarios. *Climatic Change*, 150(3–4), 131–147. <https://doi.org/10.1007/s10584-018-2246-7>.
- Bunn, A.G. (2008) A dendrochronology program library in R (dplR). *Dendrochronologia*, 26, 115–124. <https://doi.org/10.1016/j.dendro.2008.01.002>.
- Burger, F., Brock, B. and Montecinos, A. (2018) Seasonal and elevational contrasts in temperature trends in Central Chile between 1979 and 2015. *Global and Planetary Change*, 162, 136–147. <https://doi.org/10.1016/j.gloplacha.2018.01.005>.
- Christie, D.A., Boninsegna, J.A., Malcolm, K., Cleaveland, A.L., Le Quesne, C., Morales, M.S., Mudelsee, M., Stahle, D.W. and Villalba, R. (2011) Aridity changes in the temperate-Mediterranean transition of the Andes since AD 1346 reconstructed from tree-rings. *Climate Dynamics*, 36, 1505–1521. <https://doi.org/10.1007/s00382-009-0723-4>.
- Cook, B.I., Anchukaitis, K.J., Touchan, R., Meko, D.M. and Cook, E.R. (2016) Spatiotemporal drought variability in the Mediterranean over the last 900 years. *Journal of Geophysical Research: Atmospheres*, 121(5), 2060–2074. <https://doi.org/10.1002/2015JD023929>.

- Cook, E.R., Briffa, K., Shiyatov, S. and Mazepa, V. (1990) Tree-ring standardization and growth trend estimation. In: Cook, E.R. and Kairiukstis, L.A. (Eds.) *Methods of Dendrochronology: Applications in the Environmental Sciences*. Dordrecht: Kluwer Academic Publishers, pp. 104–162.
- Čufar, K., de Luis, M., Eckstein, D. and Kajfez-Bogataj, L. (2008) Reconstructing dry and wet summers in SE Slovenia from oak tree-ring series. *International Journal of Biometeorology*, 52, 607–615. <https://doi.org/10.1007/s00484-008-0153-8>.
- Danandeh Mehr, A. and Vaheddoost, B. (2020) Identification of the trends associated with the SPI and SPEI indices across Ankara, Turkey. *Theoretical and Applied Climatology*, 139, 1531–1542. <https://doi.org/10.1007/s00704-019-03071-9>.
- Erfanian, A., Wang, G. and Fomenko, L. (2017) Unprecedented drought over tropical South America in 2016: significantly under-predicted by tropical SST. *Scientific Reports*, 7, 5811. <https://doi.org/10.1038/s41598-017-05373-2>.
- Escobedo, C. and Sarricolea, P. (2017) Análisis y tendencias de la irregularidad temporal y espacial de la precipitación en Chile mediterráneo, período 1965–2010. *Cuadernos Geográficos*, 56 (3), 26–43.
- Fang, K., Chen, F., Sen, A.K., Davi, N., Huang, W., Li, J. and Seppä, H. (2014) Hydroclimate variations in central and monsoonal Asia over the past 700 years. *PLoS One*, 9(8), e102751. <https://doi.org/10.1371/journal.pone.0102751>.
- Fernández, A., Muñoz, A., González-Reyes, Á., Aguilera-Betti, I., Toledo, I., Puchi, P., Sauchyn, D., Crespo, S., Frene, C., Mundo, I., González, M. and Vignola, R. (2018) Dendrohydrology and water resources management in south-central Chile: lessons from the Río Imperial streamflow reconstruction. *Hydrology and Earth System Science*, 22, 2921–2935. <https://doi.org/10.5194/hess-22-2921-2018>.
- Flantua, S.G.A., Hooghiemstra, H., Vuille, M., Behling, H., Carson, J. F., Gosling, W.D., Hoyos, I., Ledru, M.P., Montoya, E., Mayle, F., Maldonado, A., Rull, V., Tonello, M.S., Whitney, B.S. and González-Arango, C. (2016) Climate variability and human impact in South America during the last 2000 years: synthesis and perspectives from pollen records. *Climate of the Past*, 12, 483–523. <https://doi.org/10.5194/cp-12-483-2016>.
- Fritts, H.C. (1976) *Tree Rings and Climate*. London: Academic Press.
- Fritts, H.C., Guiot, J., Gordon, G.A. and Schweingruber, F. (1990) Methods of calibration, verification, and reconstruction. In: Cook, E.R. and Kairiukstis, L.A. (Eds.) *Methods of Dendrochronology: Applications in the Environmental Sciences*. Dordrecht: Kluwer Academic Publishers, pp. 104–162.
- Garreaud, R., Boisier, J.P., Rondanelli, R., Montecinos, A., Sepúlveda, H.H. and Veloso-Aguila, D. (2020) The Central Chile mega drought (2010–2018): a climate dynamics perspective. *International Journal of Climatology*, 40(1), 421–439. <https://doi.org/10.1002/joc.6219>.
- Garreaud, R.D., Alvarez-Garretón, C., Barichivich, J., Boisier, J.P., Christie, D., Galleguillos, M., Le Quesne, C., McPhee, J. and Zambrano-Bigiarini, M. (2017) The 2010–2015 megadrought in Central Chile: impacts on regional hydroclimate and vegetation. *Hydrology and Earth System Science*, 21, 6307–6327. <https://doi.org/10.5194/hess-21-6307-2017>.
- Garreaud, R.D., Vuille, M., Compagnucci, R.H. and Marengo, J. (2009) Present-day south American climate. *Palaeogeography, Palaeoclimatology, Palaeoecology*, 281, 180–195. <https://doi.org/10.1016/j.palaeo.2007.10.032>.
- González, M.E., Gómez-González, S., Lara, A., Garreaud, R. and Díaz-Hormazábal, I. (2018) The 2010–2015 Megadrought and its influence on the fire regime in central and south-central Chile. *Ecosphere*, 9 e02300. <https://doi.org/10.1002/ecs2.2300>.
- González-Reyes, A. (2016) Ocurrencia de eventos de sequías en la ciudad de Santiago de Chile desde mediados del siglo XIX. *Revista de Geografía Norte Grande*, 64, 21–32.
- González-Reyes, A., McPhee, J., Christie, D.A., Le Quesne, C., Szejner, P., Masiokas, M.H., Villalba, R., Muñoz, A.A. and Crespo, S. (2017) Spatiotemporal variations in hydroclimate across the Mediterranean Andes (30°–37°S) since the early twentieth century. *Journal of Hydrometeorology*, 18(7), 1929–1942. <https://doi.org/10.1175/JHM-D-16-0004.1>.
- Grissino-Mayer, H.D. and Fritts, H.C. (1997) The International Tree-Ring Data Bank: an enhanced global database serving the global scientific community. *The Holocene*, 7(2), 235–238.
- Holmes, R.L. (1983) Computer-assisted quality control in tree-ring dating and measurement. *Tree-Ring Bulletin*, 43, 69–78.
- Jana, P., Torrejón, F., Araneda, A. and Stehr, A. (2019) Drought periods during 18th century in central Chile (33° S): a historical reconstruction perspective revisiting Vicuña Mackenna's work. *International Journal of Climatology*, 39(3), 1748–1755. <https://doi.org/10.1002/joc.5884>.
- Kiem, S. and Verdon-Kidd, D.C. (2013) The importance of understanding drivers of hydroclimatic variability for robust flood risk planning in the coastal zone. *Australasia Journal of Water Resources*, 17(2), 126–134. <https://doi.org/10.7158/W13-015.2013.17.2>.
- LaMarche, V.C. (1978) Tree-ring evidence of past climatic variability. *Nature*, 276, 334–338. <https://doi.org/10.1038/276334a0>.
- LaMarche, V.C., Holmes, R.L., Dunwiddie, P.W. and Drew, L.G. (1979) *Tree-ring Chronologies of the Southern Hemisphere. Chronology Series V, Vol. 2*. Tucson: Laboratory of Tree-Ring Research, University of Arizona.
- Lara, A., Villalba, R. and Urrutia, R. (2008) A 400-year tree-ring record of the Puelo River summer-fall streamflow in the Valdivian Rainforest eco-region, Chile. *Climatic Change*, 86, 331e356–331e356. <https://doi.org/10.1007/s10584-007-9287-7>.
- Larsson, L.A. (2012) CoRecorder & CDendro program. Cybis Elektronik & Data AB. Version 8.1.
- Le Quesne, C., Stahle, D.W., Cleaveland, M.K., Therrell, M.D., Aravena, J.C. Barichivich, J. (2006) Ancient Austrocedrus tree-ring chronologies used to reconstruct Central Chile precipitation variability from A.D. 1200 to 2000. *Journal of Climate*, 19, 5731–5744. <https://doi.org/10.1175/JCLI3935.1>.
- Le Quesne, C., Acuña, C., Boninsegna, J.A., Rivera, A. and Barichivich, J. (2009) Long-term glacier variations in the Central Andes of Argentina and Chile, inferred from historical records and tree-ring reconstructed precipitation. *Palaeogeography, Palaeoclimatology, Palaeoecology*, 281, 334–344. <https://doi.org/10.1016/j.palaeo.2008.01.039>.
- Ljungqvist, F.C., Piermattei, A., Seim, A., Krusic, P.J., Büntgen, U., He, M., Kirdayanov, A.V., Luterbacher, J., Schenider, L., Seftingen, K., Stahle, D.W., Villalba, R., Yang, B. and Esper, J. (2019) Ranking of tree-ring based hydroclimate reconstructions of the past millennium. *Quaternary Science Reviews*, 230, 106074. <https://doi.org/10.1016/j.quascirev.2019.106074>.

- Ma, Y., Liu, Y., Song, H., Sun, J., Lei, Y. and Wang, Y. (2015) A standardized precipitation evapotranspiration index reconstruction in the Taihe Mountains using tree-ring widths for the last 283 years. *PLoS One*, 10(7), e0133605. <https://doi.org/10.1371/journal.pone.0133605>.
- Mantua, N.J. and Hare, S.R. (2002) The Pacific decadal oscillation. *Journal of Oceanography*, 58, 35–44. <https://doi.org/10.1023/A:1015820616384>.
- Masiokas, M.H., Villalba, R., Christie, D.A., Betman, E., Luckman, B.H., Le Quesne, C., Prieto, M.R. and Mauget, S. (2012) Snowpack variations since AD 1150 in the Andes of Chile and Argentina (30°–37°S) inferred from rainfall, tree-ring and documentary records. *Journal of Geophysical Research*, 117, D05112. <https://doi.org/10.1029/2011JD016748>.
- McKee, T.B., Doesken, N.J., Kleist, J. (1993) *The Relationship of Drought Frequency and Duration to Time Scales. Preprints, Eighth Conference on Applied Climatology, Anaheim, CA, American Meteorological Society*, pp. 179–184.
- Meseguer-Ruiz, O., Ponce-Philimon, P.I., Quispe-Jofré, A.S., Guijarro, J.A. and Sarricolea, P. (2018) Spatial behaviour of daily observed extreme temperatures in Northern Chile (1966–2015): data quality, warming trends, and its orographic and latitudinal effects. *Stochastic Environmental Research Risk Assessment*, 32(12), 3503–3523. <https://doi.org/10.1007/s00477-018-1557-6>.
- Meza, J. (2013) Recent trends and ENSO influence on droughts in Northern Chile: an application of the Standardized Precipitation Evapotranspiration Index. *Weather and Climate Extremes*, 1, 51–58. <https://doi.org/10.1016/j.wace.2013.07.002>.
- Montecinos, A. and Aceituno, P. (2003) Seasonality of the ENSO-related rainfall variability in Central Chile and associated circulation anomalies. *Journal of Climate*, 16, 281–296. [https://doi.org/10.1175/1520-0442\(2003\)016%3C0281:SOTERR%3E2.0.CO;2](https://doi.org/10.1175/1520-0442(2003)016%3C0281:SOTERR%3E2.0.CO;2).
- Morales, M.S., Christie, D.A., Villalba, R., Argollo, J., Pacajes, J., Silva, J.S., Alvarez, C.A., Llancabure, J.C. and Soliz Gamboa, C. C. (2012) Precipitation changes in the South American Altiplano since 1300 AD reconstructed by tree-rings. *Climate of the Past*, 8, 653–666. <https://doi.org/10.5194/cp-8-653-2012>.
- Mundo, I.A., Masiokas, M.H., Villalba, R., Morales, M.S., Neukom, R., Le Quesne, C., Urrutia, R.B. and Lara, A. (2012) Multi-century tree-ring based reconstruction of the Neuquén River streamflow, northern Patagonia, Argentina. *Climate of the Past*, 8, 815–829. <https://doi.org/10.5194/cp-8-815-2012>.
- Olmstead, S.M. (2010) The economics of managing scarce water resources. *Review of Environmental Economics Policy*, 4(2), 179–198. <https://doi.org/10.1093/reep/req004>.
- Piticar, A. (2018) Changes in heat waves in Chile. *Global and Planetary Change*, 169, 234–246. <https://doi.org/10.1016/j.gloplacha.2018.08.007>.
- Prieto, M. (2016) Practicing costumbres and the decommodification of nature: the Chilean water markets and the Atacameño people. *Geoforum*, 77, 28–39. <https://doi.org/10.1016/j.geoforum.2016.10.004>.
- Prieto, M.R., Araneo, D., Villalba, R., (2010). The Great Droughts of 1924–25 and 1968–69 in the Argentinean Central Andes: Socio-economic impacts and responses, *II International Symposium “Reconstructing Climate Variations in South America and the Antarctic Peninsula over the last 2000 years”*, CIN-Facultad de Ciencias Forestales y Recursos Naturales, UACH-PAGES, Valdivia, Chile, 57 pp.
- Quintana, J.M. and Aceituno, P. (2012) Changes in the rainfall regime along the extratropical west coast of South America (Chile): 30–43°S. *Atmosfera*, 25(1), 1–22.
- Razavi, S. and Vogel, R. (2018) Prewhitening of hydroclimatic time series? Implications for inferred change and variability across time scales. *Journal of Hydrology*, 557, 109–115. <https://doi.org/10.1016/j.jhydrol.2017.11.053>.
- Rinn, F. (2005) *TSAPWinTM – Time series analysis and presentation for dendrochronology and related applications. Version 4.69*.
- Rondanelli, R., Hatchett, B., Rutllant, J., Bozkurt, D. and Garreaud, R. (2019) Strongest MJO on record triggers extreme Atacama rainfall and warmth in Antarctica. *Geophysical Research Letters*, 46, 3482–3491. <https://doi.org/10.1029/2018GL081475>.
- Rutllant, J. and Fuenzalida, H. (1991) Synoptic aspects of the Central Chile rainfall variability associated with the southern oscillation. *International Journal of Climatology*, 11, 63–76.
- Sarricolea, P. and Meseguer-Ruiz, O. (2015) Sequias en Chile central a partir de diferentes índices en el período 1981–2010. *Investigaciones Geográficas Chile*, 50, 19–32. <https://doi.org/10.5354/0719-5370.2015.41178>.
- Sarricolea, P., Meseguer-Ruiz, O., Martín-Vide, J. and Outeiro, L. (2018) Trends in the frequency of synoptic types in Central-Southern Chile in the period 1961–2012 using the Jenkinson and Collinson synoptic classification. *Theoretical and Applied Climatology*, 134, 193–204. <https://doi.org/10.1007/s00704-017-2268-5>.
- Sarricolea, P., Serrano-Notivoli, P., Fuentealba, M., Hernández-Mora, M., de la Barrera, F., Smith, P. and Meseguer-Ruiz, O. (2020) Recent wildfires in Central Chile: detecting links between burned areas and population exposure in the wildland urban interface. *Science of the Total Environment*, 706(135984), 135894. <https://doi.org/10.1016/j.scitotenv.2019.135894>.
- Saurral, R.I., Camilloni, I.A. and Barros, R. (2017) Low-frequency variability and trends in centennial precipitation stations in southern South America. *International Journal of Climatology*, 37(4), 1774–1793. <https://doi.org/10.1002/joc.4810>.
- Seftigen, K., Björklund, J., Cook, E.R. and Linderholm, H.W. (2015) A tree-ring field reconstruction of Fennoscandian summer hydroclimate variability for the last millennium. *Climate Dynamics*, 44, 3141–3154. <https://doi.org/10.1007/s00382-014-2191-8>.
- Spinioni, J., Barbosa, P., De Jager, A., McCormick, N., Naumann, G., Vogt, J.V., Magni, D., Masante, D. and Mazzeschi, M. (2019) A new global database of meteorological drought events from 1951 to 2016. *Journal of Hydrology: Regional Studies*, 22, 100593. <https://doi.org/10.1016/j.ejrh.2019.100593>.
- Stokes, M.A. and Smiley, T.L. (1968) *An Introduction to Tree-Ring Dating*, 2nd edition. Tucson: The University of Arizona Press.
- Stolpe, N. and Undurraga, P. (2016) Long term climatic trends in Chile and effects on soil moisture and temperature regimes. *Chilean Journal of Agricultural Research*, 76(4), 487–496. <https://doi.org/10.4067/S0718-58392016000400013>.
- Tejedor, E., Saz, M.A., Esper, J., Cuadrat, J.M. and de Luis, M. (2017) Summer drought reconstruction in northeastern Spain inferred from a tree ring latewood network since 1734. *Geophysical Research Letters*, 44(16), 8492–8500. <https://doi.org/10.1002/2017GL074748>.
- Thornthwaite, C.W. (1948) An approach toward a rational classification of climate. *Geographical Review*, 38, 55–94.

- Trenberth, K.E. (1997) The definition of El Niño. *Bulletin of the American Meteorological Society*, 78(12), 2771–2777. [https://doi.org/10.1175/1520-0477\(1997\)078%3C2771:TDOENO%3E2.0.CO;2](https://doi.org/10.1175/1520-0477(1997)078%3C2771:TDOENO%3E2.0.CO;2).
- Urrutia, R.B., Lara, A., Villalba, R., Christie, D.A., Le Quesne, C. and Cuq, A. (2011) Multicentury tree ring reconstruction of annual streamflow for the Maule River watershed in south central Chile. *Water Resources Research*, 47, W06527. <https://doi.org/10.1029/2010WR009562>.
- Valdés-Pineda, R., Cañón, J. and Valdés, J.B. (2018) Multi-decadal 40- to 60-year cycles of precipitation variability in Chile (South America) and their relationship to the AMO and PDO signals. *Journal of Hydrology*, 556, 1153–1170. <https://doi.org/10.1016/j.jhydrol.2017.01.031>.
- Valdés-Pineda, R., Valdés, J.B., Diaz, H.F. and Pizarro-Tapia, R. (2016) Analysis of spatio-temporal changes in annual and seasonal precipitation variability in South America-Chile and related ocean–atmosphere circulation patterns. *International Journal of Climatology*, 36, 2979–3001. <https://doi.org/10.1002/joc.4532>.
- Veldkamp, T.I.E., Wada, Y., Aerts, J.C.J.H. and Ward, P.J. (2006) Towards a global water scarcity risk assessment framework: incorporation of probability distributions and hydro-climatic variability. *Environmental Research Letters*, 11, 024006 <https://doi.org/10.1088/1748-9326/11/2/024006>.
- Vicente-Serrano, S.M., Beguería, S. and López-Moreno, J.I. (2010) A multiscalar drought index sensitive to global warming: the standardized precipitation evapotranspiration index. *Journal of Climate*, 23, 1696–1718. <https://doi.org/10.1175/2009JCLI2909.1>.
- Vicuña-Mackenna, B. (1877) *Ensayo histórico sobre el clima de Chile (desde los tiempos prehistóricos hasta el gran temporal de julio de 1877)*. Valparaíso: Imprenta del Mercurio.
- Vuille, M. and Milana, J.P. (2007) High-latitude forcing of regional aridification along the subtropical west coast of South America. *Geophysical Research Letters*, 34, L23703 <https://doi.org/10.1029/2007GL031899>.
- Wigley, T.M.L., Briffa, K. and Jones, P.D. (1984) On the average value of correlated time series, with applications in dendroclimatology and hydrometeorology. *Journal of Applied Meteorology and Climatology*, 23, 201–213.
- Wilhite, D.A. and Glantz, M.H. (1985) Understanding: the drought phenomenon: the role of definitions. *Water International*, 10 (3), 111–120.
- Zambrano, F., Vrieling, A., Nelson, A., Meroni, M. and Tadesse, T. (2018) Prediction of drought-induced reduction of agricultural productivity in Chile from MODIS, rainfall estimates, and climate oscillation indices. *Remote Sensing of Environment*, 219, 15–30. <https://doi.org/10.1016/j.rse.2018.10.006>.
- Zhao, Y., Shi, J., Shi, S., Yu, J. and Lu, H. (2017) Tree-ring latewood width based July–august SPEI reconstruction in South China since 1888 and its possible connection with ENSO. *Journal of Meteorological Research*, 31, 39–48. <https://doi.org/10.1007/s13351-017-6096-4>.

How to cite this article: Serrano-Notivoli R, Tejedor E, Sarricolea P, *et al.* Hydroclimatic variability in Santiago (Chile) since the 16th century. *Int J Climatol.* 2020;1–16. <https://doi.org/10.1002/joc.6828>